This article has been accepted for publication in IEEE/OSA Journal of Lightwave Technology. This is the author's version which has not been fully edited and content may change prior to final publication. Citation information: DOI 10.1109/JLT.2022.3169209



# Coherent EML+TIA Detector for DSP-Free 1 Gb/s/λ Reception Over Extended Budget

Nemanja Vokić, *Member, IEEE,* Dinka Milovančev, *Member, IEEE,*
Fotini Karinou, *Member, IEEE,* Bernhard Schrenk, *Member, IEEE*

***Abstract*— The continuing drive towards broadband access necessitates cost-effective optical access and mobile fronthaul solutions. While the fixed-mobile convergence motivates high-speeds for the antenna remoting through broadband digitized radio-over-fiber, the access segment still uses time division multiplexed access equipment. Although the steadily increasing line rates call for 50 Gb/s solutions, the unshared per-user rate remains in the 1-Gb/s range. It is a question whether such data rate can be facilitated without high-speed components, at the same time supporting higher passive splits for the optical distribution networks. We experimentally demonstrate a simplified receiver based on an electro-absorption modulated laser, co-integrated on a die-level with a transimpedance amplifier. We investigate its sensitivity for the phase-agnostic coherent heterodyne downstream detection of data signals in a passive optical network scenario. We will show that despite the omission of a high-performance local oscillator, balanced detection and digital signal processing, the proposed receiver accomplishes reception of 1 Gb/s phase-modulated signals over a link reach of 57 km and an optical budget of 48 dB, thus enabling high passive splits of 1:128. We study the implications raised by this single-ended coherent receiver architecture under multi-channel transmission and investigate the susceptibility of its integrated local oscillator to optical feedback.**

***Index Terms*— Optical communication terminals, Optical signal detection, Optical fiber communication**

## I. Introduction

COHERENT passive optical network (PON) technologies have been in the focus of research for more than a decade. This effort is well justified when looking at the two primary performance offerings that could be potentially harvested for successfully transferring coherent technology, originally developed for the metro-core domain, to the shorter-reach access segment [1]: Unshared per-user data rates of 1 Gb/s and above can be easily guaranteed through virtual point-to-point pipes enabled by ultra-dense wavelength division multiplexing (WDM), while at the same time high optical budgets for the optical distribution network (ODN) can be easily overcome by virtue of higher reception sensitivities.

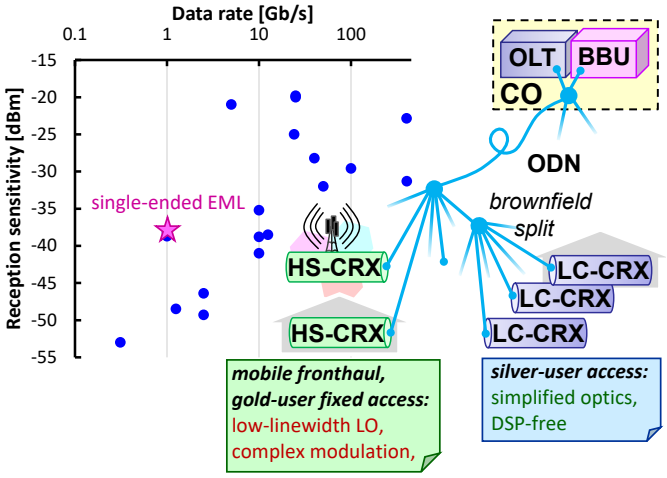


Fig. 1. State-of-the-art demonstrations for coherent PON and reference architecture featuring high-speed coherent receivers (HS-CRX) for the mobile fronthaul and low-complexity coherent receivers (LC-CRX) for wired access.

However, coherent optics is also well known for the higher cost that results from its more complex physical-layer sub-systems – an impediment that does not bode well with a cost-sensitive segment such as optical broadband access networks. Optical network units (ONU) do not adhere to cost sharing models since – in contrary to metro-access – an exclusive per-user dedication applies to the tail-end communication equipment. A techno-economic roadblock is therefore often faced due to the complexity of coherent transceivers as they often require a high-performance local oscillator (LO), increased optical or radio frequency (RF) port count, or means of digital signal processing (DSP) to assist signal recovery [2].

A plethora of research works has investigated various options to simplify coherent transceivers, with the ultimate goal to support a migration of optical access from direct to coherent detection [1, 3-8]. Early works proposed phase-diversity receivers [9], which aimed at easing linewidth and phase-locking requirements; however, DSP is still necessary as well as complex optical components such as a 90° hybrid. More recent approaches include DSP-free coherent receivers [10-13]. Those works typically employ polarization beam splitters (PBS), and require multiple photodetectors. In [14], the authors eliminate the need for PBS, but the architectural

Manuscript received January 5, 2022. This work was supported in part by the European Research Council (ERC) under the European Union's Horizon 2020 research and innovation programme (grant agreement No 804769).

N. Vokić, D. Milovančev and B. Schrenk are with the AIT Austrian Institute of Technology, Center for Digital Safety&Security, Giefinggasse 4, 1210 Vienna, Austria (phone: +43 50550-4131; fax: -4150; e-mail: bernhard.schrenk@ait.ac.at).

F. Karinou is with Microsoft Research Ltd, Cambridge, CB1 2FB, United Kingdom (e-mail: fotini.karinou@microsoft.com).

TABLE I
COHERENT PON DEMONSTRATIONS

| Ref. | TX | Modulation | Detection scheme | RX | Sensitivity | Loss budget | Reach |
|---|---|---|---|---|---|---|---|
| [1] JLT'17 | I/Q modulator | DQPSK | Intradyne | 90° hybrid, 2×balanced PIN | -49.3 dBm @ 1.25 Gbaud, BER=$3.8\times10^{-3}$ | 43 dB | 80 km |
| [19] JOCN'20 | ECL + dual-pol. I/Q modulator | QPSK | Heterodyne | ECL/DFB LO + coupler + balanced PIN | -29.6 dBm @ 50 GBaud, BER=$4\times10^{-3}$ | 36.6 dB | 20 km ($2^8$ users) 40 km ($2^7$ users) 60 km ($2^6$ users) 80 km ($2^4$ users) |
| [6] JLT'20 | Intensity modulator | OOK | Intradyne | LO + PBS + 3×3 coupler + 3 PIN PDs and envelope detectors | -48.5 dBm @ 1.25 Gb/s, BER = $2\times10^{-3}$ | - | - |
| [20] JLT'20 | EML | OOK | Heterodyne | LO + coupler + PBS + 2 (free-running) PIN PDs + 2 TIAs + 2 envelope detectors | -20 dBm (b2b) -13.7 dBm (40 km) @ 25 Gb/s, BER = $5\times10^{-5}$ | - | 40 km |
| [8] OFC'19 | Uncooled DFB / ECL + dual-pol. I/Q modulator | DQPSK | Homodyne | Comb laser as an LO + PBS + full-field receiver | -25 dBm @ 12 Gbaud, BER=$4.4\times10^{-3}$ | - | - |
| [22] OFC'20 | ECL + PBS + 2×MZM | 4-PAM | Heterodyne | LO (ECL) + coupler + PIN PD | -32 dBm @ 25 Gbaud, BER=$3.8\times10^{-3}$ | 40 dB | 20 km / 50 km |
| [18] OFC'19 | ECL + pol. mux + MZM + EDFA | PDM 4-PAM | Heterodyne | ECL + pol. div. hybrid + 2 balanced PIN PDs | -20 dBm @ 50 Gbaud, BER=$1\times10^{-2}$ | 29 dB | 20 km |
| [21] OFC'20 | Low-linewidth laser + dual-pol. I/Q modulator | 4D 256-ary | Intradyne | Low-linewidth LO + full-field receiver | -31.3 dBm @ 28 Gbaud, BER=$5\times10^{-3}$ | 31.3 dB | - |
| [17] PTL'19 | EML + dual-pol. I/Q modulator | DP-16-QAM | Intradyne | full-field receiver | -22.85 dBm @ 400 Gb/s, BER=$1.8\times10^{-8}$ | 13.4 dB | 40 km |
| *this work* | DFB + MZM | BPSK | Heterodyne | EML | -38.2 dBm @ 1Gb/s, BER=$3.8\times10^{-3}$ | 48 dB | 58 km |

Abbreviations used in the table: (D)QPSK (differential) quaternary phase shift keying, ECL external cavity laser, EDFA Erbium-doped fiber amplifier, I/Q inphase/quadrature, OOK on-off keying, PAM pulse amplitude modulation, PBS polarization beam splitter, PD photodetector, PDM polarization division multiplexing, QAM quaternary amplitude modulation

complexity with three photodetector branches still remains.

In contrast to those developments of simplified coherent receivers, the more recently investigated integration of mobile fronthaul links calls for >50 Gb/s rates at a very much reduced sensitivity. It therefore permits, to some degree, the use of coherent optics associated to a higher complexity and tailored to the specific needs of fiber-wireless convergence [2, 15-22].

The reception sensitivity of intensity-modulated direct-detection receivers can be increased by pre-amplifying the optical signal using a semiconductor optical amplifier (SOA), such as presented in [23], or by using avalanche- instead of pin photodetectors [24]. However, the direct-detection approach fails to offer inherent channel selection, as opposed to coherent detection, thus complicating the deployment in power-splitting optical distribution networks.

In this work, which is aiming at simplified coherent detection, we extend a recent work on a receiver for multi-carrier radio signals [25] and experimentally demonstrate a broadband coherent PON receiver based on the co-integration of an O-band electro-absorption modulated laser (EML) and a transimpedance amplifier (TIA). By doing so, we obtain a low-complexity analogue receiver with a sufficiently wide bandwidth for coherent heterodyne detection of a 1-Gb/s phase-modulated data signal. A reception sensitivity of -38 dBm is accomplished for this single-ended, EML+TIA based coherent receiver.

The paper is organized as follows. Section II positions the current work within the state-of-the-art research on coherent access. Section III presents the concepts underpinning the EML+TIA receiver and Section IV discusses the EML+TIA prototype assembly used in this work. Section V provides a characterization of the proposed coherent receiver, which is introduced to the evaluation environment as highlighted in Section VI. The experimental results for signal transmission are discussed in Section VII. Finally, Section VIII concludes the work.

## II. COHERENT OPTICS FOR PON AND MOBILE FRONTHAUL

The accomplishments of recent state-of-the-art works on coherent reception for next-generation PON and digital mobile fronthaul applications are summarized in Fig. 1 and Table I. Originally, the drive towards ultra-dense WDM PONs [26] was motivated by colorless architectures for their ODN and massive power splits in the order of 1:128, while further enabling an extended reach of 80 km. Considering the C-band end-of-life fiber loss of ITU-T G.652B compatible single-mode fiber, both together lead to an immense optical budget of ~54 dB. Although remarkable achievements such as a 311 Mb/s/user data rate with a sensitivity of -53 dBm [3] have

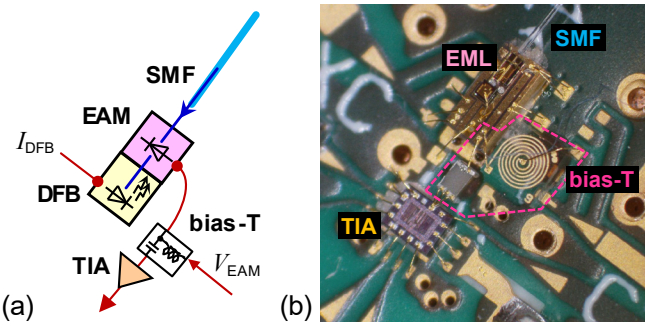


Fig. 2. (a) EML+TIA receiver architecture and (b) assembly.

been demonstrated towards this direction, this performance challenge, together with the implications of a multi-channel wavelength feed in λ-per-user broadcast architectures, renders the practical implementation of coherent systems as a complex technical task – especially in view of the cost-sensitivity of optical access and the maturity of colorless coherent components. Therefore, TDM-based solutions have prevailed for the symmetric bandwidth provisioning of up to 1 Gb/s per user [27].

With the ongoing fiber-wireless convergence and the adoption of cloud-based radio access network, a maximum ODN reach of ~20 km is now considered due to 5G latency requirements. This would reduce the optical budget for coherent PON architectures to 37.5 dB – a target that is feasible in light of recent demonstrations of up to 10 Gb/s/λ (Fig. 1). Moreover, the introduction of small-cell architectures that strive for higher data rates calls for 50G high-speed PON [28]. Nonetheless, the architectural co-existence with PON technologies integrated at the same fiber plant and aiming at virtual point-to-point WDM over power-split ODN (Fig. 1) underpins that the question for low-complexity coherent PON solutions is still timely and pressing [5]. This is because optical spectrum remains as an abundant resource in the field of short-reach networks and the time-sharing of a "gold-class" 50G PON among many users connected to a 1:64 brown-field split still results in a per-user rate of less than 1 Gb/s, while at the same time it would require high-speed transceiver components at the customer premises.

The present work therefore investigates a single-ended EML as low-complexity "silver-class" receiver (Fig. 1) that assists the coherent signal reception. In contrary to very recent coherent access demonstrations that aim to optimize the data rate rather than the sensitivity, the main objective is to investigate the sensitivity improvement in the 1 Gb/s per-user regime, while keeping the physical layer realization as lean as possible, thus omitting any form of high-performance LO, balanced detection with increased port-count, or means of DSP.

## III. Coherent EML-Inspired PON Receiver

Figure 2(a) presents the conceptual layout of the analogue coherent receiver at the optical network units (ONU) of the PON. The EML is commonly used as a transmitter, where the distributed feedback (DFB) laser acts as an emitter, and the electroabsorption modulator (EAM) section as a modulator. Conversely, the EML can be used for a photoreception. Such receiver design originates from an earlier proposal [29] that conducts coherent detection by beating an LO and an optical data signal in an EAM. The EAM photodiode receives the incoming modulated light signal, and the DFB section acts as an LO in a monolithic EML configuration. This arrangement has been demonstrated to enable homodyne detection by virtue of a transparently operated EAM photodiode, resulting in an injection-locked LO [29] so to yield a fully analogue coherent receiver. In contrast, the present investigation will exploit the arrangement where the local emission is spaced from the incident optical field by a desired intermediate frequency (IF) which is larger than the locking range of the EML, for the purpose of heterodyne detection of a phase-modulated data signal and its down-conversion to an IF at the electrical domain [30]. This heterodyne detection scheme further simplifies the ONU receiver as it omits the phase-diversity mixer in the optical domain otherwise required for intradyne reception, thus relaxing the number of photoelectric converters, RF interfaces and the requirements for a narrow LO linewidth. However, the IF rises with the bandwidth of the data signal. This, in turn, necessitates a large opto-electronic bandwidth for the coherent receiver. A wide and flat bandwidth that accommodates the heterodyne detection of Gb/s data signals has yet not been demonstrated for EML-based coherent receivers with a TIA-based front-end. Towards this direction, the present work extends the findings from our earlier works [25, 29].

It shall be stressed that a single-ended, single-polarization design will be experimentally evaluated in Sections V to VII. This is due to the use of a common die-level EML device. However, polarization-independent operation of such an EML-inspired coherent receiver has been validated earlier [31] and shall therefore not constitute a roadblock for practical deployment. Moreover, it shall be noted that the use of an EAM photodiode that can be alternatively used as an electro-optic modulator provides means to facilitate full-duplex signal transmission [32].

The availability of an analogue coherent receiver ensures a greatly simplified, DSP-free ONU, while it further enables a filterless PON architecture, provided that the EML can be widely tuned with respect to its emission frequency [33]. It shall be stressed that an approach with a statistical-wavelength LO comprising of a limited-tunability laser source can be alternatively applied. In such a deployment scheme, inventory stock issues concerning the emission wavelengths of optical sources are avoided by assigning a random rather than a pre-determined wavelength to the LOs, thus forming an ultra-dense WDM PON with statistical wavelength allocation per user. As reported recently [34], even low-cost DFB lasers with limited tuning range as low as about 3 nm can be used in a 256-user flexible ultra-dense WDM PON with experimentally demonstrated channel spacings of 6.25 and 12.5 GHz, by dynamically allocating their wavelengths, using only coarse thermal tuning.

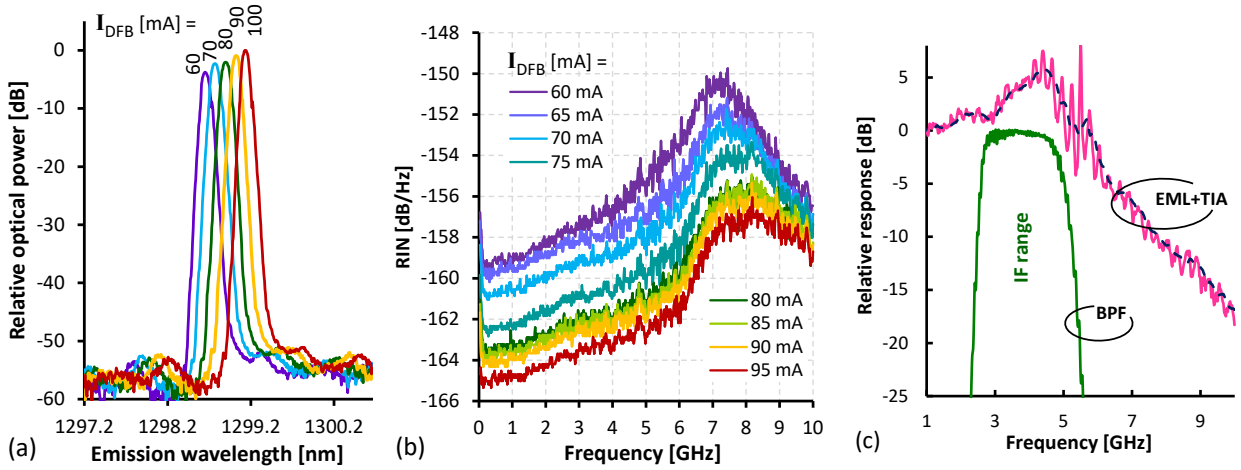


Fig. 3. (a) Relative EML emission spectrum at 28°C. (b) RIN spectrum of the LO at 28°C. (c) Frequency response of the EML+TIA receiver and IF range determined by the used bandpass filter (BPF).

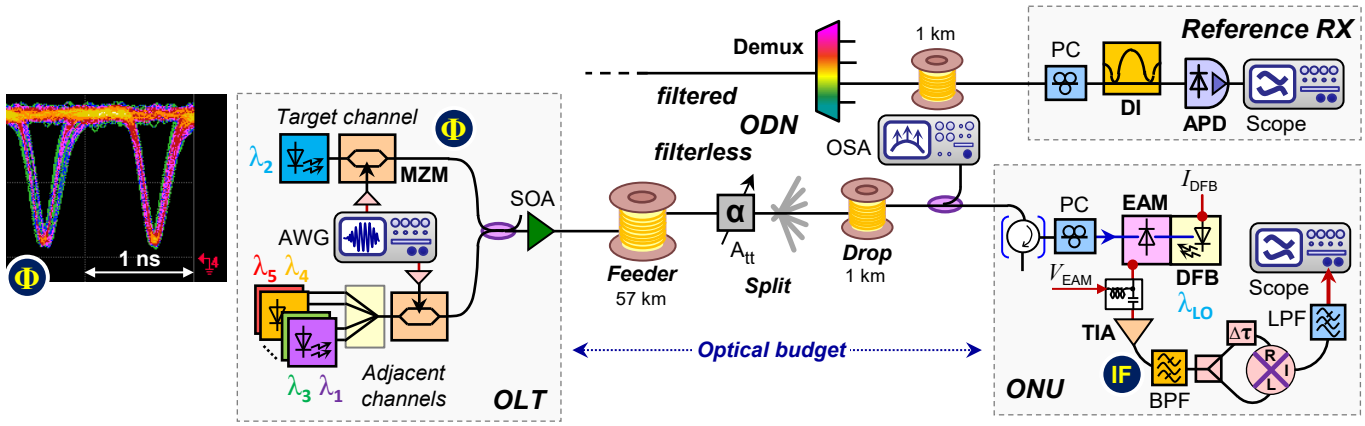


Fig. 4. Experimental setup used to evaluate coherent downstream reception and reference architecture with filtered ODN and direct-detection receiver.

## IV. EML+TIA Assembly

The coherent receiver assembly is presented in Fig. 2(b). We have employed a chip-on-carrier EML rated for transmission data rates up to 28 Gb/s for local area network (LAN) WDM applications at the O-band. The choice of the O-band was therefore solely reasoned by the available of EML device. The photocurrent generated within the EAM photodiode was amplified and converted to a voltage signal by a die-level TIA. The used TIA had a -3 dB bandwidth rated at 9 GHz for a photodetector capacitance of 220 fF. With both components, EML and TIA, building on die-level rather than packaged components, the corresponding parasitics are omitted and stability of the receiver circuit is ensured. However, as will be shown shortly, the measured TIA bandwidth is smaller than the rated bandwidth due to the additional parasitic components of an additionally required ac-coupling capacitor: Since the EAM photocurrent consists of a large dc component due to the LO beat term, EML and TIA had to be ac-coupled using a bondable 10-nF capacitor, whereas the dc current was extracted before the TIA input through a bondable inductor. This RF bias-tee in the signal path is also highlighted in Fig. 2(b). Due to the relatively low inductance of this bondable inductor, a wideband discrete bias-tee was added to the EAM bias branch.

## V. Characterization of the EML+TIA Receiver

The O-band EML used at the coherent receiver featured a low threshold current of 13 mA. The fiber-coupled power was 7.3 dBm for a DFB bias current of 90 mA and an unbiased EAM section. The side-mode suppression ratio was more than 50 dB, as reported through the normalized optical emission spectrum in Fig. 3(a). Spectral tuning of the DFB emission can be accomplished through adjustment of its bias current or the EML temperature. The corresponding tuning efficiencies were characterized with 2.26 GHz/mA and 11.8 GHz/°C, respectively, by acquiring the optical emission spectrum of the EML while changing the DFB bias current and temperature of the EML in steps of 10 mA and 0.5°C, respectively. Both affect the refractive index of the DFB cavity, thus leading to a change in emission frequency for the LO employed in the EML-based coherent heterodyne receiver. The EAM extincts the light emission by 20.3 dB at a reverse bias of 2 V.

Since the EML is employed in a single-ended detector configuration, there are no means for common-mode rejection such as it would apply for a balanced detector. It is therefore paramount for the LO to feature a low relative intensity noise (RIN). The corresponding RIN characteristics are presented in Fig. 3(b). At a DFB bias of 95 mA, the RIN remains below 157 dB/Hz. It shows an enhancement around 8.2 GHz, which is attributed to the relaxation oscillations of the DFB laser.

This article has been accepted for publication in IEEE/OSA Journal of Lightwave Technology. This is the author's version which has not been fully edited and content may change prior to final publication. Citation information: DOI 10.1109/JLT.2022.3169209



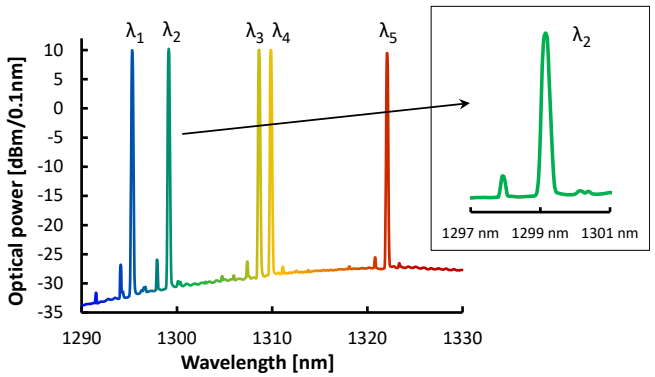


Fig. 5. Transmitted optical downstream spectrum.

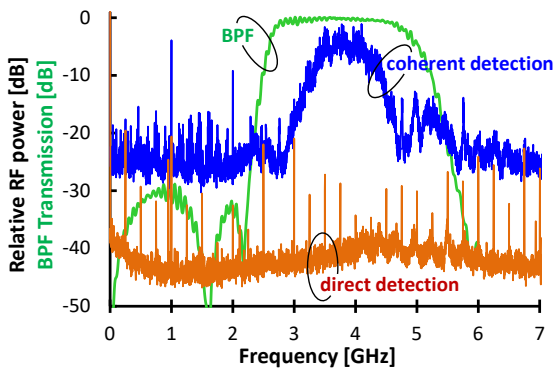


Fig. 6. RF spectrum of the BPSK signal after coherent heterodyne detection.

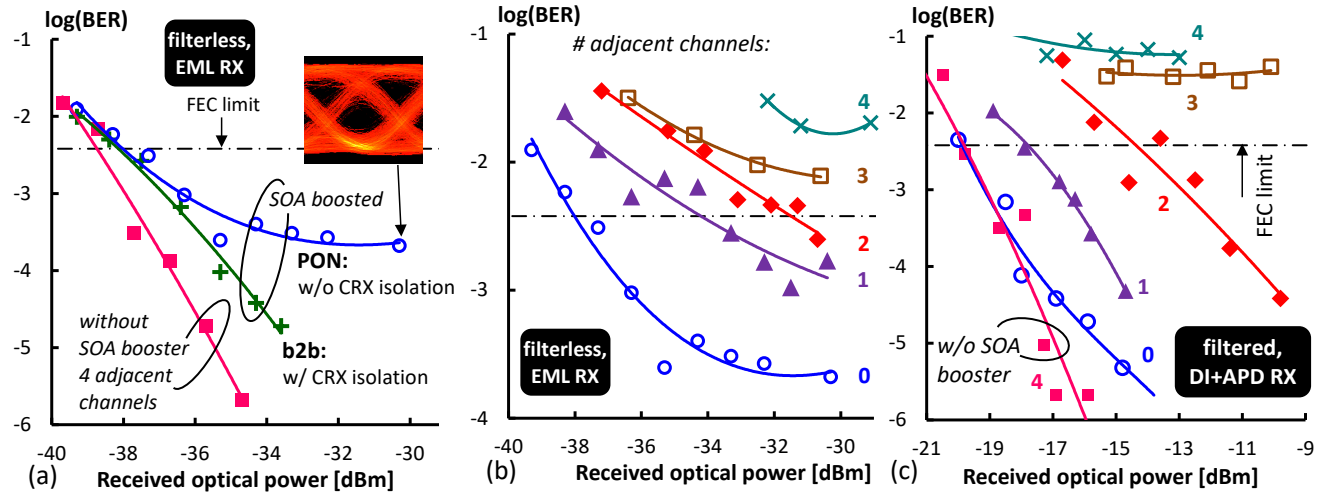


Fig. 7. (a) Single-channel BER performance for back-to-back transmission and over a filterless PON using the EML receiver. The inset shows the received eye diagram of the PON configuration at -30.3 dBm of input optical power. (b) BER performance for PON transmission when appending adjacent data channels for SOA-boosted launch from the CO. (c) Comparison with DI+APD receiver and filtered PON.

Concerning the EAM-TIA detector configuration, Fig. 3(c) shows that the actually measured receiver bandwidth was 6.1 GHz. This reduction from its rated value arises due to the additional parasitic components of the bondable elements forming the RF bias-tee to extract the dc photocurrent arising from the LO beat term. It is expected that the bandwidth can be extended through a custom TIA design that addresses this large dc term inherent to coherent receivers. Nevertheless, the accomplished EML+TIA bandwidth allows for the phase-agnostic yet bandwidth-inefficient heterodyne detection of the 1 Gbaud heterodyne BPSK data signal, which requires an opto-electronic bandwidth with a higher cut-off at ~3 times the data symbol rate [30].

## VI. Experimental Setup

The experimental setup that resembles the scenario of a coherent PON downlink is presented in Fig. 4. A 1-Gbaud symbol stream is modulated as binary phase shift keying (BPSK) signal on an O-band wavelength of 1299.15 nm ($\lambda_2$) using a Mach-Zehnder modulator (MZM) and a modulation swing of $2V_\pi$ biased at the null point. The transmitted eye diagram shown in inset Φ of Fig. 4 is monitored after the MZM using a wideband (20 GHz) benchtop PIN photodetector. Four modulated adjacent channels ($\lambda_1$, $\lambda_3$, $\lambda_4$, $\lambda_5$) at 1295.3, 1308.6, 1309.85 and 1322.05 nm are surrounding the target channel at $\lambda_2$. The compound O-band signal at a level of -10.5 dBm/λ is then boosted by a SOA due to the unavailability of an O-band doped fiber amplifier and launched with a spectrally uniform optical power level of 10 dBm/λ and an optical signal-to-noise ratio of 40.8 dB/0.1nm at $\lambda_2$. Figure 5 reports the corresponding signal spectrum as it is transmitted by the optical line terminal (OLT). At the ONU side, the optical signal is detected by the EAM. The EAM also receives a continuous wave light from the DFB acting as an LO, which is spaced by 4 GHz from $\lambda_2$, in order to enable a heterodyne detection. Practical coherent PONs would allocate the adjacent data channels in the vicinity of the target channel, ideally with a spacing as small as possible yet without incurring crosstalk during downstream detection, while also facilitating upstream transmission [1]. However, due to inventory issues concerning the available O-band sources and due to the primary focus on the EML+TIA assembly rather than on PON deployment studies, the O-band channels in the present experiment are spaced remotely from the target channel. Nevertheless, due to inherent channel selectivity provided by coherent reception, we believe that a closer spacing of channels should not have a negative impact, provided that the electrical reception bandwidth of the EML+TIA receiver is carefully chosen with respect to the grid

channel spacing. This reasoning is expanded in Section VII.

The ODN was composed of a 57-km feeder span with ITU-T G.652B compatible single-mode fiber (SMF), a power-splitting stage emulated by a variable optical attenuator ($A_{tt}$) and a 1-km drop fiber. The kilometric fiber transmission loss at the O-band target channel wavelength was 0.424 dB/km.

The ONU receiver builds on the single-ended EML+TIA receiver with integrated LO. The input polarization was manually aligned with a polarization controller (PC) at the EML input. This controller can be omitted by incorporating a polarization diversity architecture for either receiver or transmitter. The EML was biased at ~90 mA for its DFB-based LO, thus close to the maximum of the permissible forward current of its DFB section, and at -0.75V for its EAM photodiode. The LO emission wavelength was tuned to down-convert the received BPSK signal to an IF centered between 3.7 and 4.4 GHz. Figure 6 shows a received data signal spectrum for the two cases of having a lit DFB section as active LO, and a dark DFB as deactivated LO. The first case corresponds to coherent reception and the BPSK signal spectrum is clearly visible at its IF, whose range is defined by the transfer function of the bandpass filter (BPF). An analogue RF demodulator is then used to down-convert the phase-modulated IF signal to the electrical baseband. Lowpass filtering (LPF) at the baseband further enhances the signal quality. Error counting is conducted after acquisition of the signal with a real-time oscilloscope. For the dark DFB, corresponding to direct detection, the received signal does not feature a signature of the data signal due to the low delivered optical power. This is evidenced by the noisy received signal spectrum in Fig. 6.

## VII. Transmission Performance

Figure 7 reports the bit error ratio (BER) upon coherent heterodyne reception, for which the received optical power to the analogue EML+TIA downstream receiver has been adjusted through the variable optical attenuator at the ODN.

Single-channel transmission at the target channel ($\lambda_2$) has been first conducted in order to evaluate the back-to-back (b2b) performance and the sensitivity to a fully furnished ODN. Figure 7(a) presents the corresponding results. An optical circulator has been preceding the EML+TIA receiver for the back-to-back measurements in order to optically isolate the coherent receiver (CRX) from optical feedback. This is of interest to investigate the stability of the LO, which in contrary to common coherent receiver architectures is submitted to optical injection from the ODN. This also applies to self-injection at an ODN that generates optical feedback from the LO emission that bleeds through the EAM. For the optically isolated back-to-back case, a sensitivity of -38.2 dBm (+) has been obtained at the hard-decision forward error correction (FEC) limit of $3.8\times10^{-3}$. When furnishing the PON with transmission fibers and power split, while removing the optical circulator preceding the EML+TIA receiver, a small penalty of 0.2 dB applies at the FEC level (○). However, a BER floor shows up due to the optical feedback at the drop fiber span to the optically active EML receiver. Nonetheless, a high optical budget of 48 dB can be facilitated with the given per-channel launch at the CO. This budget covers a passive split of 1:128, together with the transmission losses of the 58-km long feeder and drop fiber spans. As such, it renders the low-complexity receiver as sensitive enough for coherent PON architectures.

Figure 7(b) reports the BER performance under filterless PON conditions (and without receiver isolation) when additional adjacent channels are lit up. Neighboring channels are leading to an additional noise contribution, which introduces a sharply rising penalty of 4.2 and 6.5 dB when co-propagating the channels at $\lambda_1$ (▲) and $\lambda_1+\lambda_3$ (◆) over the PON. The BER is already exceeding the FEC limit for 3 and 4 adjacent channels (□,×). Although it could be inferred that this penalty is due to the missing common-mode noise suppression of the single-ended EML receiver, the penalty is attributed to cross-modulation arising at the booster amplifier of the OLT: bypassing this SOA-based amplifier eliminates the observed penalty, as it is evidenced in Fig. 7(a) through the 5-channel unamplified transmission (■). The improvement with respect to the amplified single-channel transmission (+) is explained by the absence of amplified spontaneous emission.

To confirm the detrimental influence of the SOA booster, a direct-detection receiver building on a 1-GHz delay interferometer (DI) and avalanche photodetector (APD) has been employed in a filtered PON configuration with a LAN-WDM demultiplexer replacing the power-splitting stage. Due to the reduced receiver sensitivity, the feeder fiber has been entirely omitted. Figure 7(c) reports the corresponding BER performance, which is similar to that found for the EML receiver: An increasing number of adjacent channels leads to a rising error floor when the SOA booster is used at the OLT (▲,◆,□,×), while the unamplified transmission (■) with 4 adjacent channels performs as good as the amplified single-channel transmission (○). Had a C-band EML been available in die form, a rare-earth doped fiber amplifier would have been employed at the OLT site instead of the SOA, in which case the amplifier-induced noise would have been greatly omitted [35]. We will leave this for future investigation.

The components of the EAM photocurrent contributed by the adjacent channels are transferred through the ac-coupling capacitor to the TIA, since these additional channels are modulated. However, the finite TIA bandwidth leads to suppression of these components, and they do not interfere electrically with the desired channel. The maximum TIA bandwidth should thus be limited by the channel spacing, such that the frequency difference between the LO (DFB section) and the optical carrier of the adjacent channel falls ideally beyond the optoelectronic bandwidth of the TIA, to avoid side-channel interference as well as saturation of the TIA. Ultimately, the electrical bandpass filtering of the analog processing circuitry is ensuring the lowest amount of noise arising from adjacent channels.

## VIII. Conclusion

An analogue coherent receiver based on a simplified EML+TIA assembly has been proposed and evaluated for

coherent heterodyne detection of 1-Gb/s BPSK signals. We have shown that the accomplished sensitivity of this low-complexity receiver supports a massive 1:128 split for an optical link with a reach of 58 km. The utilized single-ended receiver design has been proven to be compatible with a filterless feed of five data channels.

Nonetheless, a balanced receiver architecture is expected to enable further improvements in terms of LO noise suppression and an ultra-dense channel broadcast. This, as well as the adoption of a polarization diversity scheme for polarization-insensitive operation, are left for future work. A custom TIA, designed for the specific values of EML circuit parasitics, and with the cancelling mechanism of input dc current – instead of using an externally bonded bias-tee – should provide a further improvement in performance, both in terms of noise and achievable data rate.

## REFERENCES


[1] A. Shahpari *et al.*, "Coherent Access: A Review," *IEEE/OSA J. Lightwave Technol.*, vol. 35., no. 4, pp. 1050-1058, Feb. 2017.

[2] Y. Zhu *et al.*, "Comparative study of cost-effective coherent and direct detection schemes for 100 Gb/s/λ PON," *IEEE/OSA J. Opt. Comm. Netw.*, vol. 12, no. 9, pp. D36-D47, Sep. 2020.

[3] S. Smolorz, E. Gottwald, H. Rohde, D. Smith, and A. Poustie, "Demonstration of a Coherent UDWDM-PON with Real-Time Processing," in *Proc. Opt. Fib. Comm. Conf. (OFC)*, Los Angeles, United States, Mar. 2011, PDPD4.

[4] K.Y. Cho *et al.*, "Long-Reach Coherent WDM PON Employing Self-Polarization-Stabilization Technique," *IEEE/OSA J. Lightwave Technol.*, vol. 29, no. 4, pp. 456-462, Feb. 2011.

[5] M.S. Erkılınç *et al.*, "Comparison of Low Complexity Coherent Receivers for UDWDM-PONs (λ-to-the-User)," *IEEE/OSA J. Lightwave Technol.*, vol. 36, no. 16, pp. 3453-3464, Aug. 2018.

[6] E. Ciaramella, "Assessment of a Polarization-Independent DSP-Free Coherent Receiver for Intensity-Modulated Signals," *IEEE/OSA J. Lightwave Technol.*, vol. 38, no. 3, pp. 676-683, Feb. 2020.

[7] J.A. Tabares, S. Ghasemi, J. C. Velásquez, and J. Prat, "Coherent Ultra-Dense WDM-PON Enabled by Complexity-Reduced Digital Transceivers," *IEEE/OSA J. Lightwave Technol.*, vol.38, no. 6, pp. 1305-1313, Mar. 2020.

[8] M.M.H. Adib *et al.*, "Colorless Coherent Passive Optical Network using a Frequency Comb Local Oscillator," in *Proc. Opt. Fib. Comm. Conf. (OFC)*, San Diego, United States, Mar. 2019, Th3F.4.

[9] A. Davis, M. Pettitt, J. King and S. Wright, "Phase diversity techniques for coherent optical receivers," *IEEE/OSA J. Lightwave Technol.*, vol. 5, no. 4, pp. 561-572, Apr. 1987.

[10] J. Tabares, V. Polo, and J. Prat, "Polarization-independent heterodyne DPSK receiver based on 3×3 coupler for cost-effective udWDM-PON," in *Proc. Opt. Fib. Commun. (OFC)*, Los Angeles, United States, Mar. 2017, Th1K.3.

[11] J. A. Altabas *et al.*, "Real-Time 10Gbps Polarization Independent Quasicoherent receiver for NG-PON2 Access Networks," in *Proc. Opt. Fiber Commun. Conf. (OFC)*, San Diego, United States, Mar. 2018, Th1A3.

[12] M. S. Erkilinc *et al.*, "Comparison of Low Complexity Coherent Receivers for UDWDM-PONs (λ-to-the-user)," *IEEE/OSA J. Lightw. Technol.*, vol. 36, no. 16, pp. 3453–3464, Aug. 2018.

[13] M. Artiglia, M. Presi, F. Bottoni, M. Rannello, and E. Ciaramella, "Polarization-Independent Coherent Real-Time Analog Receiver for PON Access Systems," *IEEE/OSA J. Lightw. Technol.*, vol. 34, no. 8, pp. 2027–2033, Apr. 2016.

[14] M. Rannello, M. Presi and E. Ciaramella, "PBS-Free Polarization-Independent PON Coherent Receiver," *IEEE Photon. Technol. Lett.*, vol. 32, no. 21, pp. 1361-1364, Nov. 2020.

[15] H.K. Shim, K.Y. Cho, U.H. Hong, and Y.C. Chung, "Transmission of 40-Gb/s QPSK upstream signal in RSOA-based coherent WDM PON using offset PDM technique," *OSA Opt. Expr.*, vol. 21, no. 3, pp. 3721-3725, Feb. 2013.

[16] N. Suzuki, H. Miura, K. Matsuda, R. Matsumoto, and K. Motoshima, "100 Gb/s to 1 Tb/s Based Coherent Passive Optical Network Technology," *IEEE/OSA J. Lightwave Technol.*, vol. 36, no. 8, pp. 1485-1491, Apr. 2018.

[17] F. Pittalà *et al.*, "400-Gbit/s DP-16-QAM Transmission Over 40-km Unamplified SSMF With Low-Cost PON Lasers," *IEEE Phot. Technol. Lett.*, vol. 31, no. 15, pp. 1229-1232, Aug. 2019.

[18] J. Zhang, H.C. Chien, Y. Cai, W. Wang, W. Zhou, and Z. Hu, "200-Gb/s/λ PDM-PAM-4 PON with 29-dB Power Budget Based on Heterodyne Coherent Detection," in *Proc. Opt. Fib. Comm. Conf. (OFC)*, San Diego, United States, Mar. 2019, Th3F.1.

[19] M. Erkılınç, R. Emmerich, K. Habel, V. Jungnickel, C. Schmidt-Langhorst, C. Schubert, and R. Freund, "PON transceiver technologies for ≥50 Gbits/s per λ: Alamouti coding and heterodyne detection [Invited]," *IEEE/OSA J. Opt. Commun. Netw.*, vol. 12, no. 2, pp. A162-A170, Feb. 2020.

[20] J. A. Altabas, O. Gallardo, G. S. Valdecasa, M. Squartecchia, T. K. Johansen, and J. B. Jensen, "DSP-Free Real-Time 25 GBPS Quasicoherent Receiver With Electrical SSB Filtering for C-Band Links up to 40 km SSMF," *IEEE/OSA J. Lightwave Technol.*, vol. 38, no. 7, pp. 1785-1788, Apr. 2020.

[21] L. Zhang, H. Chien, Y. Cai, W. Wang, W. Zhou, and Z. Hu, "Four-Dimensional 8-Bit Modulation with KP4 Non-Binary FEC for Short-Reach Coherent Optical Transmissions," in *Proc. Opt. Fib. Comm. Conf. (OFC)*, San Diego, United States, Mar. 2020, Th2A.47.

[22] H. Li, M. Luo, X. Li, and S. Yu, "Demonstration of 50-Gb/s/λ PAM-4 PON with Single-PD using Polarization-Insensitive and SSBI Suppressed Heterodyne Coherent Detection," in *Proc. Opt. Fib. Comm. Conf. (OFC)*, San Diego, United States, Mar. 2020, Th1B.4.

[23] T. Kimura, S. Bjorlin, Hsu-Feng Chou, Qi Chen, Shaomin Wu, and J. E. Bowers, "Optically preamplified receiver at 10, 20, and 40 Gb/s using a 1550-nm vertical-cavity SOA," *IEEE Phot. Technol. Lett.*, vol. 17, no. 2, pp. 456-458, Feb. 2005.

[24] J. Yamada, A. Kawana, T. Miya, H. Nagai, and T. Kimura, "Gigabit/s Optical Receiver Sensitivity and Zero-Dispersion Single-Mode Fiber Transmission at 1.55 μm," *IEEE Trans. Microw. Theory Techn.*, vol. 30, no. 10, pp. 1525-1535, Oct. 1982.

[25] D. Milovančev, N. Vokić, F. Karinou, and B. Schrenk, "Simplified Coherent Receiver for Analogue Radio Transmission Over High Optical Budgets", *IEEE/OSA J. Lightwave Technol.*, vol. 39, no. 24, pp. 7672-7681, Dec. 2021.

[26] D. Lavery *et al.*, "Opportunities for Optical Access Network Transceivers Beyond OOK [Invited]," *IEEE/OSA J. Opt. Comm. Netw.*, vol. 11, no. 2, pp. A186-A195, Feb. 2019.

[27] R. Sánchez, J.A. Hernández, J. Montalvo García, and D. Larrabeiti, "Provisioning 1 Gb/s Symmetrical Services with Next-Generation Passive Optical Network Technologies," *IEEE Comm. Mag.*, vol. 54, no. 2, pp. 72-77, Feb 2016.

[28] V. Houtsma, A. Mahadevan, N. Kaneda, and D. van Veen, "Transceiver technologies for passive optical networks: past, present, and future [Invited Tutorial]," *IEEE/OSA J. Opt. Comm. Netw.*, vol. 13, no. 1, pp. A44-A55, Jan. 2021.

[29] B. Schrenk, "Injection-Locked Coherent Reception Through Externally Modulated Laser," *IEEE J. Sel. Topics in Quantum Electron.*, vol. 24, no. 2, p. 3900207, 2018.

[30] A.W. Davis *et al*., "Phase Diversity Techniques for Coherent Optical Receivers," *IEEE/OSA J. Lightwave Technol.*, vol. 5, no. 4, pp. 561-571, Apr. 1987.

[31] B. Schrenk, and F. Karinou, "Simple Laser Transmitter Pair as Polarization-Independent Coherent Homodyne Detector," *OSA Opt. Expr.*, vol. 27, no. 10, pp. 13942-13950, 2019.

[32] B. Schrenk, and F. Karinou, "A Coherent Homodyne TO-Can Transceiver as Simple as an EML," *IEEE/OSA J. Lightwave Technol.*, vol. 37, no. 2, 555-561, Jan. 2019.

[33] T. Tanbun-Ek et al., "Broad-Band Tunable Electroabsorption Modulated Laser for WDM Application," *IEEE J. Sel. Topics in Quantum Electron.*, vol. 3, no. 3, pp. 960-967, Jun. 1997.

[34] J. Segarra, V. Sales, V. Polo, J. Tabares, and J. Prat, "Flexible coherent UDWDM-PON with dynamic user allocation based on limited-tunability lasers," *IEEE/OSA J. Opt. Commun. Netw.*, vol. 12, no. 9, pp. D27-D35, Sep. 2020.

[35] A.W. Setiawan Putra, M. Yamada, S. Ambran, T. Maruyama, "Theoretical Comparison of Noise Characteristics in Semiconductor and Fiber Optical Amplifiers," *IEEE Photon. Technol. Lett.*, vol. 30, no. 8, pp. 756-759, Apr. 2018.